Wide-temperature-range dielectric response of the charge-density-wave system TaS_3

D. Starešinić and K. Biljaković
Institute of Physics, P.O. Box 304, HR-10001 Zagreb, Croatia

W. Brütting and K. Hosseini
Experimental Physics II, University of Bayreuth, 95440 Bayreuth, Germany

P. Monceau
Centre de Recherches sur les Très Basses Températures, Laboratoire Associé à l' Université Joseph Fourier, CNRS, BP 166, 38042 Grenoble Cedex 9, France

H. Berger and F. Levy
Institut de Physique Appliquée, EPFL, CH-1015, Lausanne, Switzerland
(Received 27 September 2001; revised manuscript received 9 January 2002; published 5 April 2002)

We present a detailed investigation of the low-frequency dielectric response of the charge-density-wave system (CDW) o-TaS_3 in wide temperature (5–300 K) and frequency (10 mHz to 100 MHz) ranges. Although our measurements agree relatively well with data performed in some restricted frequency and temperature ranges and previously published by several groups, we show that they do not correspond to a single low-frequency process. Instead, three distinctive processes are found to contribute to the dielectric function below the CDW transition temperature. The temperature evolution of the characteristic relaxation time of the three processes bears a close resemblance to the phenomenology of the dielectric response of glasses. The freezing of some of these processes at finite temperatures leads to changes in the CDW properties, as is thoroughly documented in the literature. Based on these results, we propose a consistent model of the temperature evolution of the CDW ground state.

DOI: 10.1103/PhysRevB.65.165109 PACS number(s): 71.45.Lr, 77.22.−d, 64.70.Pf

I. INTRODUCTION

A charge density wave[1,2] (CDW) is a spatial modulation of the density of conduction electrons, accompanied by a slight crystal lattice distortion. It is usually found in systems with a specific shape of the Fermi surface that forms parallel sheets, as, for instance, in quasi-one-dimensional (Q1D) materials. The coherent superposition of electron-hole pairs from opposite sheets coupled by the $2k_F$ (k_F being the Fermi wave vector) phonons results in a macroscopic condensed state. It is stabilized at a finite temperature called the Peierls transition temperature (T_P). Below T_P a gap opens at the Fermi level, changing the conduction properties from metallic to semiconducting. The gap, the electron modulation, and the lattice distortion can be described by a complex order parameter. Two types of excitations of the order parameter have been recognized: opticlike excitations of the amplitude (so-called amplitons) and acousticlike excitations of phase (so-called phasons). Temporal variation of the phase in the external electric field (CDW sliding) increases the conductivity above the free carrier contribution, which is known as the CDW current.

The CDW has emerged from the many-body theory treatment of pure one-dimensional electron-phonon systems as the preferable ground state at zero temperature.[3] Although it has been proposed initially to be the mechanism responsible for the superconductivity, its strictly one-dimensional nature rendered it a purely hypothetical mathematical construction. Until the number of both organic and inorganic materials exhibiting a CDW superstructure[4] has been synthesized in the 1970s. These materials are highly anisotropic, both structurally and electronically, and they undergo a transition to the CDW state with a new $2k_F$ periodicity, as has been seen in various diffraction experiments.[5] In addition, a number of new phenomena that have not been predicted by simple theoretical considerations have emerged. Different observations, such as the need for a finite electric field (so-called threshold field E_T) for the CDW sliding, the resonance in the dielectric response at finite frequency, and the narrow-band noise (NBN) observed in the sliding regime have been related to pinning of CDW phase to a preferred position.[4] Among various mechanisms proposed to account for pinning, such as commensurability, contact, or surface pinning, the idea of the interaction with impurities prevailed as the result of intensive experimental[4] and theoretical[6] work. In particular, the dependence of E_T on the impurity concentration has been decisive in this respect.

Disorder related to the impurity pinning has also provided a natural explanation for the broadband noise observed in the sliding regime, as well as different hysteretic phenomena and hours-long relaxation in the dc conductivity measurements.[4] In addition, impurities are responsible for the finite correlation length of the CDW phase and the formation of phase-coherent domains, so-called Lee-Rice (LR) domains.[6] The domain structure in the CDW superstructure, sensitive to radiation damage, has been observed in the dark-field electron microscopy,[7] although it has not been directly associated with the LR domains.

The temperature evolution of the nonlinear conductivity[8] and the existence of a strongly temperature-dependent di-

electric relaxation process below the pinning resonance[9–12] have shown that screening of the CDW by free carriers has to be considered too. And, actually, the model of a spatially dependent complex order parameter, the CDW phase being elastically distorted in order to minimize the effects of pinning and screened by free carriers[13] can account for most of the CDW phenomena observed in a large temperature range below T_P, typically between T_P and $T_P/2$ or $T_P/3$.

However, many measurements have shown that the properties of CDW systems change at lower temperatures. In fact, these changes are so drastic, although not discontinuous, that we believe that they represent different CDW ground states. This conclusion is based on various results that we have collected from the literature. In particular we shall briefly review them for one of the most studied semiconducting CDW system, *o*-TaS_3, where *o* stands for ''orthorhombic.''

o-TaS_3 undergoes a Peierls transition at $T_P=210$ K. Down to 100 K, its properties can be well described with elastic distortions of the CDW phase and screening. A first change occurs in the region between 100 K and 50 K. It includes a plateau in the linear conductivity[14,15] bridging between two regions of activated behavior, the high-temperature-activated energy being less or equal to half of the CDW gap and the low-temperature-activated energy about 2 times smaller. Next, below about 70 K, the onset of the slight nonlinearity in the *I-V* characteristics is observed below the sharp threshold E_T of the CDW sliding.[15,16] This is usually described as a new threshold field, E_T'. This second threshold field is even better resolved on lowering temperature as it decreases while E_T increases substantially. In about the same temperature region the ratio of the NBN frequency and the current carried by the sliding CDW, f_{NBN}/I_{CDW}, starts to increase.[16] This has been attributed to the stiffening of the CDW,[16] and the same mechanism could explain the increase of the pinning frequency below 100 K measured in microwave dielectric spectroscopy.[17] In the same temperature region the amplitude of the low-frequency dielectric process decreases sharply and its characteristic relaxation time goes from an activated increase to saturation.[10] The subsequent dielectric measurements at lower temperatures have shown that there is in fact a minimum at about 40 K and that the dielectric permittivity increases again below it.[18,19] The thermal hysteresis present below T_P closes.[20,21] at about 50 K, accompanied by strong fluctuations of the linear conductivity,[22] similar to the fluctuations[23] around T_P. In the same temperature range the stress dependence of the linear conductivity disappears.[24] By adding that the thermopower changes sign[25,26] at 70 K and the shear compliance has been shown to decrease substantially[27] below 50 K, we have exhausted the phenomena pointing to the change of the CDW properties around 70 K ($\approx T_P/3$).

However, there are evidences that another change occurs at even lower temperatures, in the 20–10 K range. First, the linear conductivity flattens even more,[15,28] and the temperature dependence is more readily described by hopping laws. The nonlinear conductivity has two regimes below 10 K, depending on the quality and the thickness of the samples.[29,30] For pure and/or thin samples it flattens completely, leading to the temperature-independent regime, while for thick and less pure samples it decreases further towards low temperatures. The low-frequency dielectric response, which has been observed to grow below 40 K, goes through a frequency-dependent maximum at about 20 K and then decreases sharply[18,19] down to 10 K. In the same temperature range the characteristic relaxation time, which has a temperature-activated dependence with about a quarter of the CDW gap activation energy (close to the linear conductivity activation energy below 50 K), starts to diverge, pointing to a finite freezing temperature[18,19] of about 13 K. This has been considered as the signature of a possible glass transition. And, finally, in the real-time dielectric relaxation, a new process has been observed below 10 K, exhibiting very weak temperature dependence.[31,32]

Although neither the changes in the 70 K range nor those in the 20–10 K range are abrupt, they nevertheless separate regions of a substantially different CDW behavior. This leads us to consider these ''transitions'' in the frame of glass transitions, which are not abrupt either, but separate ground states different in many important aspects. This approach has already been proposed in[18,19] for *o*-TaS_3. It has been initiated by the results of the measurements of the thermal capacity,[33,34] which have shown many similarities with low-temperature features of glasses together with the so-called ageing effect.[35] However, the CDW superstructure is hardly expected to significantly influence the thermal capacity governed by lattice dynamics above liquid helium temperatures, where the changes described above occur. Therefore the thermodynamic methods typically used for detecting a glass transition may not be so powerful as a way for seeing it in CDW systems. On the other hand, the second most used method in glass systems is dielectric spectroscopy. For the CDW systems—they being superdielectrics—this method seemed promising. More so, dielectric spectroscopy can provide the temperature evolution of the dielectric response in addition to the detection of the glass transition temperature.

Therefore we have undertaken a systematic investigation of the dielectric response of *o*-TaS_3 in a wide frequency and temperature range, paying a particular attention to the transition regions. In particular, for one sample we have been able to collect a complete set of data ranging from above T_P down to liquid helium temperature. This has been essential in obtaining consistent information on the temperature evolution of the CDW dynamics in *o*-TaS_3.

II. EXPERIMENTAL METHODS

We have measured the dielectric response of *o*-TaS_3 in the frequency range from about 100 MHz down to 10 mHz. To cover such a wide frequency range we have had to use several measuring techniques. A suitable experimental setup corresponding to the peculiarities of the technique had to be used for each of them. Furthermore, as we wanted to cover a wide range of temperatures from room temperature down to liquid helium temperature, it imposed further demands on the experimental setup and also some constraints on the range of the measurements. Below is given a short review on all the devices and setups that we have used with a brief description of the measuring procedure and limits for each of them.

In our measurements we have used three different instruments to access different frequency ranges. The impedance analyzer HP4291B (HP stands for Hewlett-Packard) covers the frequency range from 1 MHz to 1.8 GHz, it can measure the impedance up to 10 $k\Omega$, using ac signal amplitudes as low as 0.2 mV. The HP4192A covers the frequency range from 5 Hz to 13 MHz and can measure the impedance up to 1 $G\Omega$, using ac signal amplitudes down to 5 mV. To increase the accuracy for impedance higher than 100 $k\Omega$ we have used homemade preamplifiers-impedance matches. TBF2 (TBF stands for Trés Basses Fréquences, and it is homemade[19] at CRTBT-CNRS, Grenoble, France) covers the frequency range from 0.3 mHz to 3 kHz and can measure impedance up to 10^{13} Ω, using signal amplitudes down to 1 mV.

In the measurements with HP4291B the sample has been glued with silver paste to the end of an air gap coaxial line of 0.5 m length. The cooling has been performed by continuous helium gas flow from the liquid helium Dewar. The temperature has been controlled by an Oxford Instruments temperature controller, using a standard proportional-integral-derivative (PID) method.

The measurements with HP4192A and TBF2 were performed using the same setup, where just the connections were repositioned from one device to the other. It increased the consistency of the results, as the sample and temperature have been the same for the two sets of data. The sample has been mounted in the two-contact–four-wire configuration at the end of four rigid coaxial conductors using silver paste. The sample holder has been introduced directly in the liquid helium Dewar, the temperature being controlled by the instrument designed at CRTBT-CNRS using the standard PID method.

III. RESULTS AND ANALYSIS

A. Sample characterization

We will present hereafter data obtained on the same o-TaS_3 sample used with different measuring techniques, as described in the previous section. The dimensions of the sample have been as follows: the cross section estimated optically under a microscope was about $S \cong 2.3\times10^{-4}$ μm^2 (15 $\mu m \times 15$ μm). For measurements below 1 MHz, the distance between evaporated indium contacts was $l_{LF} = 3.7$ mm. In the frequency range above 1 MHz where a coaxial line was used, the length was determined by the distance of about 2 mm between the inner and outer conductors, and therefore $l_{HF} = 2$ mm. The room-temperature resistance in the two cases was $R_{RT} = 54$ Ω (below 1 MHz) and $R_{RT} = 23$ Ω (above 1 MHz). It is quite a good match considering that the silver paint contact resistance can vary from 1 Ω to 10 Ω, as measured in four-contact measurements. On the other hand, we have checked in four-contact measurements that, at least down to about 30 K, the contact resistance does not change, so below T_P it can be considered as negligible. Thus comparison of the resistance value from the two setups allows an estimate of the relative geometrical (or scaling) factor. Direct comparison of the complex conductivity yields a scaling factor of about 2, which corresponds nicely to the factor obtained directly from the length ratio of 1.85. The room-temperature resistivity estimated from the sample dimensions and R_{RT} is 2.7×10^{-6} Ω m for measurements above 1 MHz and 3.4×10^{-6} Ω m for measurements below 1 MHz, which is also in a good accordance with the value of 3.2×10^{-6} Ω m quoted in the literature.

For measurements at higher frequencies using HP 4291B, the frequency range was 10^6–2×10^8 Hz and the temperature range 295–80 K. The restriction in the frequency range available with this impedance meter was due to the appearance of a spurious resonance at about 500 MHz; on the other hand, the temperature range has been limited by the increase of the resistance of our samples beyond the instrument limits at lower temperatures. We have also measured another sample of similar dimensions (room-temperature resistance $R_{RT} = 17$ Ω) from the same batch with no significant difference in the results. The low-frequency response was measured using HP 4192A in the frequency range 400–10^6 Hz and TBF2 in the frequency range 10^{-2}–10^3 Hz, in the temperature range 150 K–5 K. The available frequency range of HP 4192A was limited by the bad resolution at low frequencies and low signal amplitudes, which we had to use in order to prevent nonlinearity in the response. On the other hand, the data above 1 MHz up to 13 MHz were discarded due to the influence of the sample holder length. The frequency range of TBF2 was restricted to above 0.01 Hz by the excessive time needed for the measurements at lower frequencies. The low-frequency dielectric spectra of two more samples were measured by these two techniques, the basic difference being only a slightly different relative amplitude of the relaxation processes observed, whereas the temperature dependence has been the same.

It is well established that the dielectric response of CDW systems in the low-frequency range depends strongly on the amplitude of the applied signal even for the values far below the threshold field.[10,36,37] Therefore we have checked this dependence at all measurements and at all temperatures, usually only for a small set of frequencies covering the whole frequency range. The data presented are obtained in the low-amplitude limit where the response did not depend on the signal amplitude.

The dielectric function will be presented in units of ϵ_0, i.e., the vacuum permittivity. This value should be taken as only an approximate one, as the geometry of the sample that enters into the evaluation of the conductivity and subsequently of the dielectric function could not be determined precisely.

B. General temperature behavior

We present in Fig. 1 the frequency dependence of the real part σ' of the complex conductivity $\sigma(\omega)$ at selected temperatures ranging from above T_P at 216 K down to 5 K.

We have achieved our goal of covering a wide temperature and frequency range. The linear dc conductivity σ_{dc} obtained from the limit $\omega \to 0$ of the low-frequency dielectric spectroscopy decreases by almost 10 orders of magnitude. At the same time the onset of the frequency-dependent conductivity shifts as well by almost 10 orders of magnitude to-

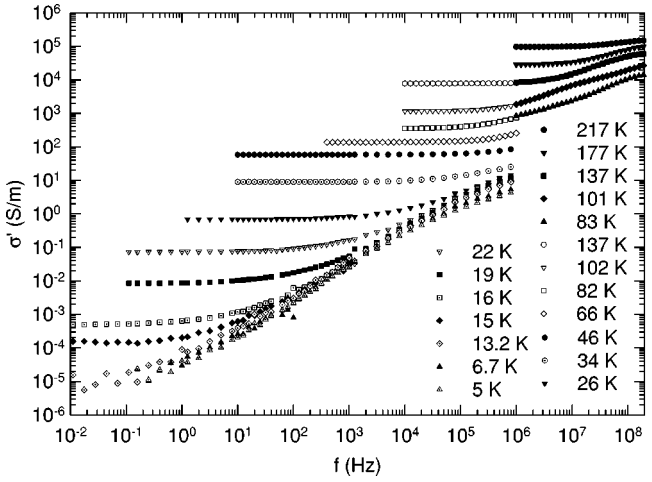

FIG. 1. Real part of the conductivity σ' of o-TaS_3 as a function of frequency at selected temperatures.

wards low frequences. This explains the need for different instruments, in conjunction with several preamplifiers, covering a wide frequency and impedance range. However, the presentation of the real part of the conductivity can be misleading, as the temperature evolution of the frequency-independent dc part can (and often does) mask the actual temperature evolution of the frequency-dependent part. Therefore, in Fig. 2 the imaginary part ϵ'' of the complex dielectric function $\epsilon(\omega)$, i.e., only the frequency-dependent dielectric response, is presented. It is calculated from the complex conductivity as

$$\epsilon(\omega)=\frac{\sigma(\omega)-\sigma_{dc}}{i\omega}. \tag{1}$$

The data in Fig. 2 reveal the ''fine structure'' of the temperature and frequency dependence. The wide maxima in the frequency dependence represent the relaxation processes. The characteristic or mean relaxation frequency ν_0 corresponds to the position of the maximum, and the characteristic relaxation time τ is the inverse of ν_0.

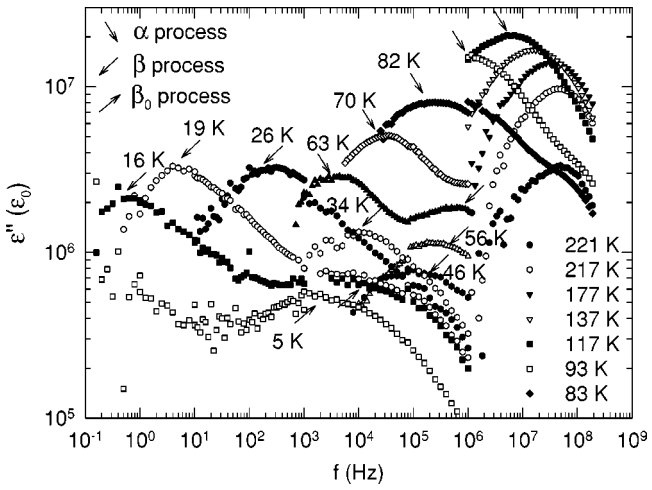

FIG. 2. Imaginary part of the dielectric function ϵ'' of o-TaS_3 as a function of frequency at selected temperatures.

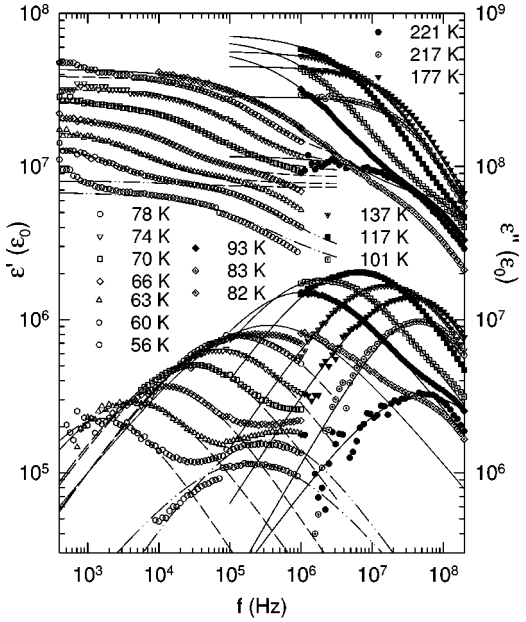

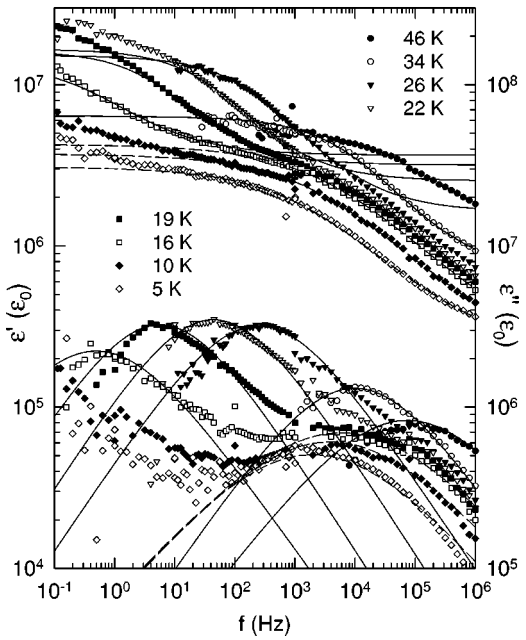

FIG. 3. Real ϵ' and imaginary ϵ'' parts of the dielectric function of o-TaS_3 as a function of frequency at several temperatures. The lines represent single-process Cole-Cole fits of the complex dielectric response data. (a) $T>50$ K: the solid lines correspond to the α process above 1 MHz, the dashed lines to the α process below 1 MHz, and the dash-dotted lines correspond to the β process seen below 60 K. (b) $T<50$ K: the solid lines correspond to the β process and the dashed lines to the β_0 process.

We can see that one relaxation process emerges already above T_P, and its temperature evolution can be followed down to about 60 K [see also Fig. 3(a)] as it gradually slows down (τ increases). In about the same temperature region another process appears at higher frequencies. We will call this second process β and the first one α in analogy with glassy systems that we will justify below. The β process is also strongly temperature dependent, as it slows down with

temperature and below 16 K actually exits our frequency window [see also Fig. 3(b)]. However, below about 25 K we can see yet another process, which we name β_0, seemingly emerging from the high-frequency tail of the β process. β_0 remains in our frequency window even at the lowest temperatures.

C. Data analysis

In order to characterize these three processes, we will use three parameters. These are the characteristic relaxation time τ which is obtained from the position of the maximum in ϵ'', the amplitude $\Delta\epsilon$ which corresponds to the difference (increase) between the high- and low-frequency frequency-independent limits of the real part of the dielectric function ϵ' (see Fig. 3), and finally the width w determined from the ratio of frequencies at which ϵ'' is at half its maximum. Some of these parameters can be extracted visually such as, for instance, τ and even w in some occasions. However, we have opted for obtaining them by numerically fitting the data to the suitable phenomenological expression. $\epsilon(\omega)$ is a complex function with the imaginary and real parts related by the Kramers-Kronig relation. Using a complex fitting function, we were able to extract from the frequency and temperature dependences of both ϵ' and ϵ'' more reliable estimates of the characteristic parameters. It actually enabled us to compensate in several occasions for the restricted frequency range (see the data at 93 K) or to distinguish the contribution of different processes (for instance, see the data at 63 K or 26 K).

For fits we have used the modified Cole-Cole function,[38] a phenomenological expression often used for describing relaxation processes in dielectric spectroscopy:

$$\epsilon(\omega)=\epsilon_{HF}+\frac{\Delta\epsilon}{1+(i\omega\tau)^{1/w}}. \tag{2}$$

Here ϵ_{HF} represents the frequency-independent ''base line'' of ϵ' at frequencies higher than the characteristic relaxation frequency ν_0. $\Delta\epsilon$ is the amplitude of the relaxation process, τ its characteristic relaxation time, and w the width in the number of decades in frequency. We use $1/w$ instead of usual notation $1-\alpha$ to avoid confusion with the α process. In Fig. 3 the temperature evolution of $\epsilon(\omega)$ is presented in detail, together with the corresponding fits.

As considerable changes in the dielectric response occur around $T\sim 50$ K, we separately show in Fig. 3(a) the temperature evolution of the α process together with the emergence of the β process below 100 K, whereas the temperature evolution of β process below 50 K including the emergence of the β_0 process is shown in Fig. 3(b). We can see clearly how the β_0 process splits from the high-frequency tail of the β process below 25 K, and although we were not able to follow continuously the temperature evolution of the β process at higher temperatures, it also seems that the β process splits from α in a very similar manner at about 100 K.

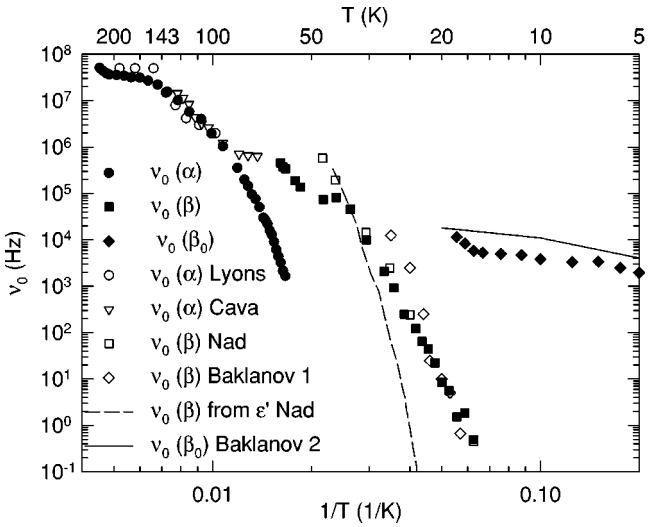

FIG. 4. Variation of the characteristic relaxation frequencies ($1/\tau$ from our dielectric spectroscopy measurements as a function of the inverse of temperature). Data previously obtained by Lyons and Tucker (Ref. 12), Cava *et al.* (Ref. 10), Nad and Moncean (Ref. 19), Baklanov *et al.* (Ref. 31), and Baklanov *et al.* (Ref. 32) are also shown for comparison.

D. Characteristic parameters

We show now in Figs. 4–6 the temperature evolution of the characteristic parameters of these three processes on a large temperature scale and compare them with data previously published in the literature.

The slowing down of all three processes is clearly seen in Fig. 4. The comparison of our results with the previously published data covering reduced temperature and frequency ranges shows a good agreement. It is clear that the distinction between the α and β processes has never been made because the measurements have not been performed in the relevant temperature region where both are present.

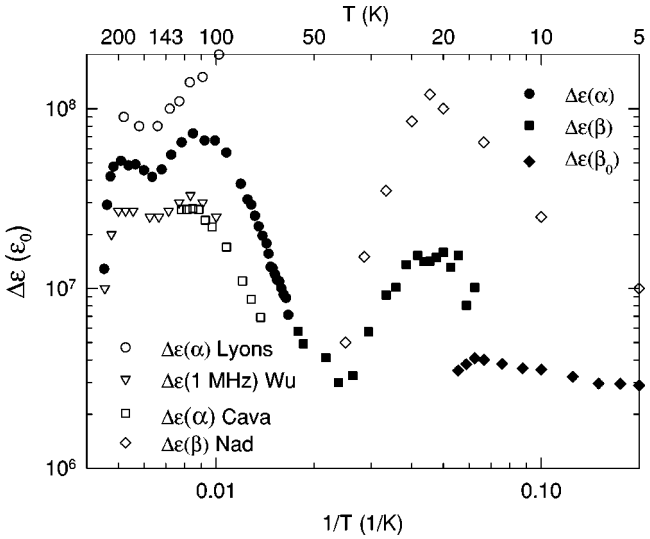

FIG. 5. Variation of the amplitude ($\Delta\epsilon$) of the three relaxation processes in dielectric relaxation as a function of the inverse temperature. Data from Lyons and Tucker (Ref. 12), Wu *et al.*, (Ref. 39), Cava *et al.*, (Ref. 10), and Nad *et al.* (Ref. 19) are also shown.

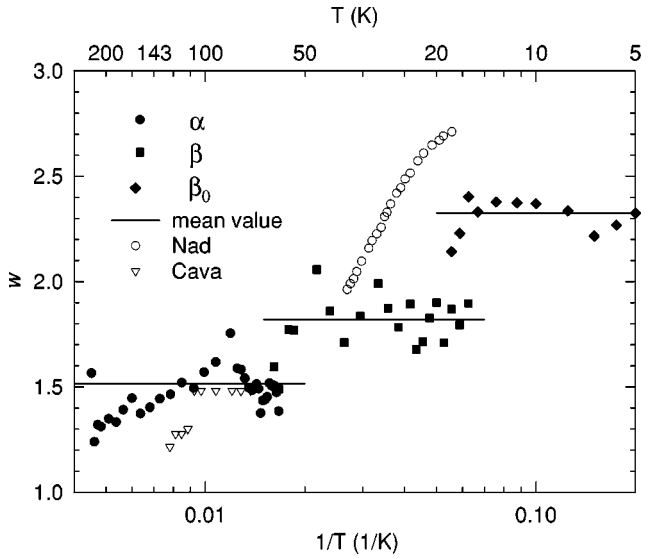

FIG. 6. Variation of the width w of the three relaxation processes as a function of the inverse of temperature, together with the data from literature [Cava *et al.* (Ref. 10), and Nad *et al.* (Ref. 19)].

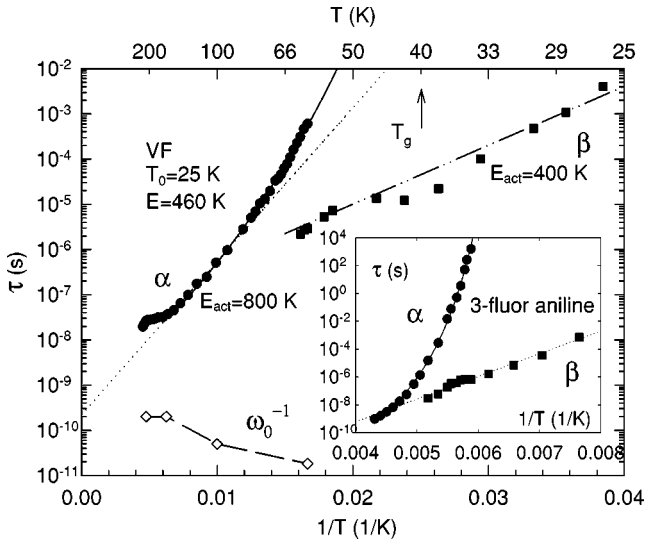

FIG. 7. Arrhenius plot of the temperature dependence of the characteristic relaxation time of α and β process observed in o-TaS_3 in the CDW state. Solid circles correspond to the pinning frequency taken from Ref. 17. The straight lines are fits to an activated growth (Ref. 41) for α and β process; the solid line represents the Vogel-Fulcher fit (Ref. 41) of the α process. The inset presents the characteristic relaxation time of α and β process in a fragile glass-forming liquid, 3-fluor aniline (Ref. 40).

The same good agreement is obtained when the amplitude of different processes is compared with the data from literature, as far as the temperature evolution is considered (Fig. 5). On the other hand, the fact that the absolute values are somewhat different is not too surprising, as the amplitude depends strongly on the impurity content.

In Fig. 6 we have drawn the temperature evolution of the width of the three relaxation processes that we have determined. It appears from our data that w seems to be characteristic for a given process. It increases in the ''hierarchy'' of the processes, from α to β_0, indicating a more disordered nature of the β and especially the β_0 process. The apparent temperature evolution of w for the α process above 100 K can be a consequence of splitting of the α process from the pinning resonance and to the splitting of the β process from α, which we will consider in more detail in the discussion. The data from the literature are sparse as only several works consider the temperature evolution of the relaxation width. The data of Ref. 10 have been obtained through a similar fitting procedure and match nicely our data. On the other hand, the data of Ref. 19 have been estimated directly from the width of the peak in imaginary part of the dielectric function. This is basically a different approach, as we have tried to distinct two processes (β and β_0) in this temperature range, whereas in Ref. 19 it is considered as a highly distributed unique process. Therefore, it is natural that this estimate should give a larger width than ours.

This is the first time that the CDW contribution to the dielectric response of o-TaS_3 at low frequencies has been shown not to be unique. Instead it comprises three distinctive processes with different characteristics. However, these processes are not completely unrelated, as it seems that they ''grow'' one from another. In the next section we will discuss our results within the phenomenology of glasses, which they resemble in some respects, and within different existing CDW models.

IV. DISCUSSION

A. Glasslike phenomenology

We will start the discussion of our results by showing the strong analogy between the temperature evolutions of the characteristic frequencies of the processes observed in our CDW system and in supercooled liquids, representative for glasses. We present the typical so-called Arrhenius plot of the relaxation time of the α and β process in Fig. 7 and of the β and β_0 process in Fig. 8. This type of plot of $\ln(\tau)$ versus $1/T$ is very convenient for strongly temperature-dependent phenomena, the straight line in the Arrhenius plot representing the thermally activated behavior. We have drawn in the inset of Fig. 7 the temperature evolution of the α and β process in 3-fluor aniline, a typical supercooled liquid system.[40] For a complete analogy with glasses, we have also shown in Fig. 7 the pinning resonance frequency of TaS_3 taken from Ref. 17.

So at first sight, the similarity between the temperature evolution of the α and β processes in our CDW system and in 3-fluor aniline is striking. In both systems the α process varies at first slowly with temperature, then shifts to a much stronger dependence as the temperature is lowered, ending eventually in a critical (faster than activated) slowing down regime before it leaves the experimentally accessible frequency window. In both systems the β process seems to split off from the high-frequency tail of the α process and then slows down gradually with a much less temperature dependence, remaining present below the temperature where the α process has disappeared.

The strong growth of the relaxation time τ of the α process leads eventually to the freezing of the α process and the

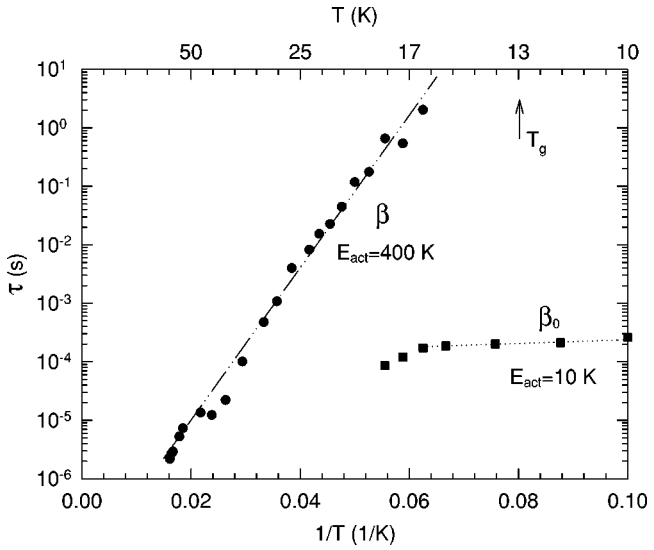

FIG. 8. Arrhenius plot of the temperature dependence of the characteristic relaxation time of the β and β_0 processes observed in o-TaS_3 in the CDW state. The lines represent the activated growth of the characteristic times (Ref. 41).

transition of the CDW system into a glass state. The freezing of a given process is defined as the regime where the characteristic relaxation time τ becomes so large that it cannot contribute to the dynamical properties of the system in any reasonable, i.e., experimentally accessible, time scale. The system is then frozen in the glass state. This state is essentially different from the high-temperature state, as many degrees of freedom associated with the frozen process are not any more accessible. Therefore they do not contribute to the phase space, which is therefore substantially reduced. The critical value of τ is conventionally defined[42] to be 10^2–10^3 s, and the temperature at which τ attains this value is consequently the temperature of the glass transition T_g. For o-TaS_3 this enables us to estimate the glass transition temperature to be about 40 K, and we would expect the properties of our system to change in this temperature range, just as is documented in the literature. The β relaxation is accordingly attributed to the remaining degrees of freedom.

There is another strong analogy between CDW systems and glass forming systems. In glasses it is found that the α process sets off as a low-frequency wing of the so-called boson peak (or resonance).[43] In CDW systems the α process sets off as the low-frequency wing of the pinning resonance (for TaS_3 see Ref. 17; for $K_{0.3}MoO_3$ see Ref. 44). We will compare the properties of these two high-frequency resonances.

In Ref. 45 two quantities characteristic for the structural correlations on the intermediate length scales for several glasses have been compared. The low-frequency Raman scattering gives the frequency ν_{max} of the boson peak, typically in the THz range. The width of the first diffraction peak in x-ray scattering gives the correlation length ξ of the disordered structure, typically of the order of few nm. Given the sound velocity v_s in these glasses, which is typically about 10^3 m/s, they have shown that for all the materials under investigation a simple relation $v_s \approx \xi \nu_{max}$ is obeyed. This leads the authors to conclude that the boson peak arises from the vibration modes of the structurally ordered units on nanometer scales.

A similar analysis can be performed for o-TaS_3. The strandlike domains seen in dark field electron microscopy,[7] which have been assigned to the instability of the CDW super-lattice, have length ξ of about 0.3 μm. The acoustic-like excitations of CDW are the phasons. The corresponding ''sound'' or phason velocity v_{ph} can be estimated from the Fermi velocity[46] $v_F \approx 10^5$ m/s and the effective CDW mass[17] $m^* \approx 10^3 m_e$ as $v_{ph} = v_F / \sqrt{m^*/m_e} \approx 3 \times 10^3$ m/s. The vibrations localized on the length scales of the CDW domains would thus have the frequency of at least 10 GHz, and the pinning resonance in TaS_3 is situated[17] at about 30 GHz. For $K_{0.3}MoO_3$ or blue bronze, this simple relation between the phase coherence volume (from x-ray diffraction[47]), directly measured phason velocity,[48] and pinning frequency[44] also holds. Therefore, we can conclude that the pinning resonance is due to localized vibration of the CDW phase ordered on the length scales of few hundreds of nanometers. It implies that we could roughly accept the domains reported in Ref. 7 as some kind of dynamical LR domains of the correlated phase.[6] Also, it establishes the CDW glass as a new type of a glass with unusually large length scales of the order of 1 μm.

The separation of α process from pinning resonance and the separation of α and β process can explain the apparent temperature dependence of the width seen in Fig. 7 above 80 K. At high temperatures the high-frequency tail of the α process is truncated by the pinning resonance, leading to the decrease of the apparent width, whereas below 100 K the emerging β process enlarges the high-frequency tail, leading to an increase of the apparent width. Only below approximately 80 K, where the two processes can be fully distinguished, does the apparent half-width of the α process resume its presumably intrinsic value of about 1.5.

Now let us consider the low-temperature regime shown in Fig. 8. This can be done from two points of view. First, the analogy posted in Fig. 7 can be continued by saying that the β_0 process is analogous to the so-called background loss,[49,50] a very wide relaxation process seen in glasses at low temperatures in the frequency range above the β process. On the other hand, one can view it separately and state that the increasing relaxation time of the β process would eventually lead to freezing (estimated to be at about 13 K) and thus to another glass transition. It resembles the scenario of the glass transition in a typical strong glass former.[42] In this case, below 13 K, the CDW would be in another ground state, which is again documented in the literature. As we have already mentioned, the glass transition due to the freezing of the β process has already been considered in Refs. 18 and 19 based also on dielectric spectroscopy data.

B. Charge-density-wave phenomenology

So far, we have established that two out of the three processes that we have observed in the dielectric spectroscopy of the CDW system o-TaS_3 freeze at finite temperatures, in the analogy with supercooled liquids. The freezing of α and

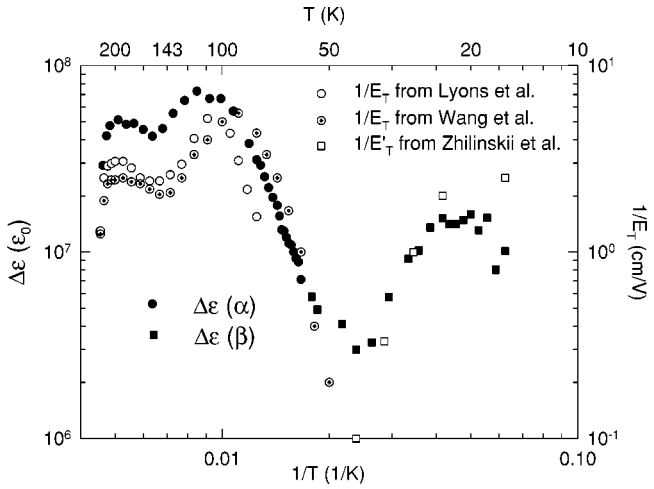

FIG. 9. Variation of the amplitude of the relaxation processes measured in o-TaS_3 as a function of the inverse of temperature, together with the inverse threshold field measured by Lyons and Tucker (Ref. 12), Zhilinskii *et al.*, (Ref. 15), and Wang *et al.* (Ref. 51).

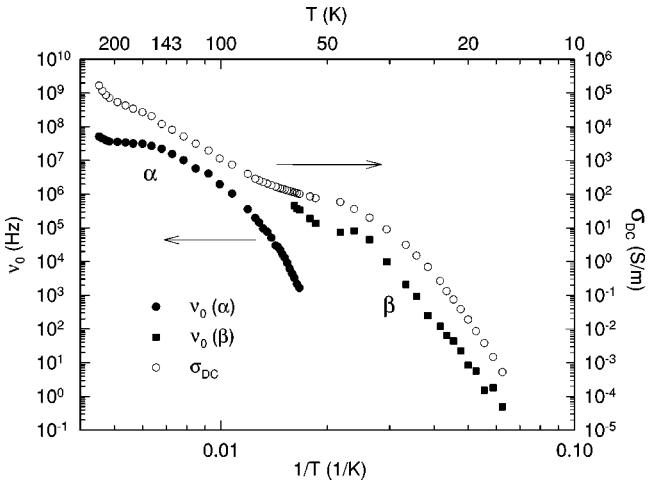

FIG. 10. Variation of the characteristic relaxation frequency of the α and β processes and of the dc conductivity as a function of the inverse of temperature in the same temperature range.

β processes below 40 K and 13 K correspondingly leads to new CDW ground states below these temperatures. Now, we will consider our results in the view of a general phenomenology of CDW systems with respect to two mechanisms that influence substantially their properties: namely, pinning by impurities and screening by free carriers.

In Fig. 9 we compare the temperature dependence of the amplitude $\Delta\epsilon$ of the α and β processes with the inverse threshold field measured in the corresponding temperature ranges (from different groups). Above 50 K the threshold field E_T for the onset of CDW sliding is presented,[12,51] whereas below 50 K the second, lower threshold field E_T' for the onset of the slight nonlinearity is given.[15] This presentation is based on the relation obtained in basically all of the CDW models considered so far (for comparison of several models see Ref. 39), stating that the dielectric permittivity multiplied by the threshold field, $\Delta\epsilon \times E_T$, should be temperature independent.

One can see in Fig. 9 that this relation applies to both the α and β processes if a different threshold field is considered, E_T for the α and E_T' for the β process. The relation $\Delta\epsilon \times E_T = \text{const}$ is a very general consequence of the CDW pinning, regardless of the details of the pinning mechanism. Therefore we can conclude that both processes represent the response of the pinned CDW, despite the fact that the CDW ground state has changed below the freezing temperature of the α process. We will have to take this fact into account when considering the appropriate microscopic model.

Next, we present in Fig. 10 the temperature evolution of the characteristic relaxation frequency ν_0 of the α and β processes together with the linear dc conductivity σ_{dc} in the chain direction. This presentation is based on the results obtained in the analysis of the dielectric response of various CDW models[52–57] that has shown either close or approximate proportionality of ν_0 and σ_{dc} due to the screening of CDW deformations by free carriers.

The temperature dependence of ν_0 for the α process $[\nu_0(\alpha)]$ follows that of σ_{dc} below 160 K (the temperature at which it splits from the pinning resonance[17]) down to about 80 K. This is also the temperature region of the activated decrease of σ_{dc}, with the activation energy being equal to half of the CDW gap opened at the Fermi level, as indicated in Fig. 7. Below 80 K, however, the temperature dependence of σ_{dc} starts to flatten towards a plateau, whereas the β process apparently splits from the α process. On the other hand, the temperature dependence of $\nu_0(\alpha)$ remains activated below 80 K (see Fig. 7) and even becomes faster than activated, as we have seen in the previous subsection, leading eventually to the freezing at finite temperature. Below approximately 50 K, σ_{dc} resumes the activated behavior, but with an activation energy that is only about one-half of the one above the plateau region. At the same temperature the temperature dependence of ν_0 of the β process $[\nu_0(\beta)]$ starts to follow closely the temperature dependence of σ_{dc} down to the lowest temperature of 16 K where it is still observable.

Obviously, both $\nu_0(\alpha)$ and $\nu_0(\beta)$ follow the temperature dependence of σ_{dc} in wide temperature regions. Even more, we can suppose that a new conducting channel is responsible for the appearance of the plateau in σ_{dc} and the subsequent activated behavior with a new activated energy, on which we will elaborate below. In this case, it is possible that the α process interacts only with the free carriers contributing to the high-temperature conducting channel and actually follows its temperature dependence even to the lowest temperatures. Therefore, we can conclude that the interaction with free carriers indeed plays an essential role in the temperature evolution of the low-frequency dielectric response of CDW subsystems in o-TaS_3, despite a different ground state below the freezing temperature of the α process.

C. Microscopic models

In this subsection we will relate our phenomenological observations from previous two subsections to the various

existing models of CDW dynamics. We will show that despite the fact that the respective processes observed could be understood within some of the models, a coherent theoretical approach that will explain a ''cascade'' of processes growing one from another still misses.

The high-temperature regime, i.e., the splitting of the α process and the pinning resonance and their subsequent temperature evolution, has been thoroughly considered in the literature.[52–55] Although different authors start from various levels of approximations, from microscopic equations[53] up to phenomenological Fukuyama-Lee-Rice model of the phase dynamics,[52] basically all the relevant theories consider only the dynamics of the CDW phase slowly varying in the disordered (impurity) pinning potential, screened by free carriers. It is shown that the inhomogeneity of the pinning potential, which leads to the formation of domains, is responsible for the low-frequency relaxation (or α) process. It enables coupling of the local (finite wavelength) excitations to the external electrical field. The dynamics of local modes is strongly influenced by the free carriers, as they screen the distortions of the phase and facilitate relaxation. Therefore, the decrease of the free carrier density with temperature (so-called descreening) is responsible for the observed slowing down of the α process. We can estimate the relevant spatial scales at which the screening is still effective; i.e., it enables the low-frequency relaxation. At the glass transition temperature $T_g \approx 40$ K the density of the free electrons estimated from the room-temperature value of about 10^{22} e/cm^3 and the activation energy of 800 K is 1 electron per 10^{-16} cm^3. It is very close to the volume of the strandlike domain obtained from dark-field electron microscopy,[7] which we have associated with the domain of the correlated CDW phase. It should be noted that we have assumed that the additional contribution to the dc conductivity responsible for the plateau does not contribute to the screening of phase deformations responsible for α process. This estimate permits us to set a *criterion for freezing* of the α process: it occurs when there is *less than one electron per the domain of the correlated CDW phase*. The microscopic CDW models should incorporate the freezing of the α process and discuss the consequences of the corresponding glass transition and the properties of the glass phase.

The inhomogeneity, or domain structure, has also been recently invoked as the origin of the low-frequency relaxation (α process) in structural glasses[58] above T_g. It would be interesting to see if the mesoscopic mean-field theory of cluster thermodynamics,[59] which naturally gives two characteristic time scales (corresponding to the α and β processes) for relaxation, as well as high-frequency overdamped resonance, can be applied to our results, and this work is under progress.

The problem of the additional contribution to the dc conductivity below 100 K has not been resolved yet. Several authors have attributed it to the thermally activated phase solitons.[15,28] They would have an appropriate activation energy[60] of $(1-2)T_P$ and would create a band within the CDW gap. On the other hand, solitons have not yet been observed despite numerous efforts, and in addition, their contribution to σ_{dc} has been estimated to decrease at low temperatures.[61] The other explanation could be that the overlap of metallic islands created around impurities at low temperatures[62] could lead to the formation of midgap states and eventually a new band. A final suggestion would be the contribution of the lattice quantum fluctuations to the CDW properties.[63] It has been shown that, due to these fluctuations, the electronic density of states extends far into the CDW gap. These states are localized and do not contribute to the free carrier current; i.e., the CDW gap edge acts as the mobility edge. However, as the states above the CDW gap are empty and those below are filled at low temperatures, the contribution of these localized states might become important, and the effective gap for dc conductivity would decrease. We believe that the relevance of these models can be tested now by that these ''new'' carriers do not couple to the local phase excitations in the weak pinning model, i.e., the α process. Important information regarding the new conduction mechanism might be the fact that it is the most pronounced in o-TaS_3 where a smooth approach of the CDW wave vector to the commensurate value has been observed in x-ray measurements[51] to take place at about 140 K. This does not necessarily lead to the locking of the CDW phase to the underlying lattice, but can instead, in the presence of impurities, result in a so-called ''rough'' phase where the overall commensurability is obtained through the proliferation of topological defects of the phase.[64]

The additional contribution to the dc conductivity is closely related to the β process, as we have shown that its temperature evolution follows the temperature evolution of the relaxation frequency of the β process. The β process has been modeled so far by the dynamics of the solitons pinned at impurities.[56,57] One of the models[56] involves the interplay of the collective (weak) pinning and the local (strong) pinning to explain the temperature evolution. As we have shown that the local modes of the weak pinning case are actually frozen at about 40 K, it seems that this model is not appropriate. The other model[57] requires the screening of solitons by the free carriers in order to explain the temperature evolution of the dielectric response and allows even that these free carriers can be the thermally activated solitons, so it might be relevant for our results. Another approach, based on the idea of the hopping of the solitons between the impurity sites, has already been proposed for an explanation of the β process.[65] It relies on the theory of the ion hopping in glasses,[66] in which both dc and ac conductivity can be related to the hopping motion, and the mean relaxation frequency appropriately scales with the dc conductivity. Recent investigation[67] relates the finite-frequency relaxation with the spatially distributed hopping motion, whereas the time-averaged hopping over large length scales leads to the dc conductivity. Even if the model of the hopping solitons can be applied, the origin of these solitons still remains unresolved. Particularly, the theories modeling the α process should also incorporate the evolution of the low-temperature state from the elastic pinned CDW through the freezing of local modes in order to get a consistent theory of the dielectric response.

Finally, there is the question of the origin of the β_0 process. The β_0 process might turn out to be very important for

the general understanding of CDW systems. It is the only process that can provide a link to the very slow CDW dynamics observed in heat relaxation[33,34] below 1 K, where the characteristic relaxation time for both α and β processes are extremely large while it would be about 1 s for the β_0 process. As it is almost temperature independent, it might be related to some kind of thermally assisted quantum tunneling, just as has been proposed for the mechanism of nonlinear conductivity of o-TaS_3 at very low temperatures.[29] A model of two-level systems[68] consisting of neutral bisolitons created at impurity sites[69–71] has been proposed to account for the low-temperature heat relaxation in both CDW and spin-density-wave (SDW) systems. It might be also applied to the β_0 process; however, the evolution of the β_0 process from β process would still be lacking.

V. CONCLUSION

We have measured the dielectric response of the CDW system o-TaS_3 in a wide temperature (5–300 K) and frequency range (from 10 mHz to 100 MHz). Our data obtained on the same sample have shown that three different relaxation processes can be observed, in contrast to the commonly accepted picture of a single response below T_P. The freezing of the α and β processes at finite temperatures gives a natural explanation for the changes of the CDW properties below the corresponding temperatures. This freezing can be viewed as the analog of the glass transition in traditional glassy systems. The comparison of the temperature dependence of the characteristic relaxation frequency and of the dc conductivity, on the one hand, and of the amplitude of the dielectric relaxation with the threshold field on the other hand suggest that both processes involve pinning of the CDW and screening of the corresponding deformations by free carriers. Comparison with the existing experimental results and theories associates the α process with the elastic pinned CDW screened by noncondensed electrons. The β process, on the other hand, is associated with the dynamics of the reduced degrees of freedom remaining after the freezing of the α process. It can be modeled by the relaxation of local, strong deformations of the CDW phase, i.e., solitons, strongly pinned to the impurities, which might be at the origin of the contribution to the dc conductivity below 50 K, too. The origin of the β_0 process that evolves from the β process is even less clear. We tentatively relate it to some kind of quantum process due to its weak temperature dependence. We can set a quantitative criterion for the freezing of the α process which occurs when screening becomes ineffective and then no longer allows the relaxation of the domains of correlated phase, namely, when there is fewer than one electron per domain.

From our results we have drawn a new and quite complex phase diagram of o-TaS_3 below the Peierls transition temperature. Similar phenomena have also been observed in other CDW's as well as in SDW materials. E.g., recent dielectric spectroscopy measurements on the CDW system $K_{0.3}MoO_3$ have also revealed the existence of the α and β processes.[72] Therefore, we consider that this new phase diagram is not unique for o-TaS_3 and that reconsiderations of theoretical CDW models at low temperatures are clearly needed. Particularly, the problem of the evolution of the β process from the α process and the β_0 process from the β process has never been considered yet.

ACKNOWLEDGMENTS

The work at the Institute of Physics in Zagreb was supported by MZT Grant No. 00350107, the work at CRTBT-CNRS in Grenoble through the French MESR network Réseau Formation-Recherche: France-Croatie and the work at the University of Bayreuth by regional Project No. IX/7-24/40 361 within Arbeitsprogramm: Bayern-Kroatien 1999-2000. We thank S. Artamenko, R. Chamberlin, K. Ngai, E. Rössler, and S. V. Zaitsev-Zotov for helpful discussions.

[1] *Electronic Properties of Inorganic Quasi-One-Dimensional Compounds*, edited by P. Monceau (Kluwer Academic, Dordrecht, 1985); G. Grüner, Rev. Mod. Phys. **60**, 1129 (1988); *Density Waves in Solids* (Addison-Wesley, New York, 1994).

[2] *Proceedings of the International Workshop on Electronic Crystals, ECRYS93, Carry-le-Rouet, France*, edited by S. Brazovskii and P. Monceau, [J. Phys. IV **3** (1993)]; *Proceedings of the International Workshop on Electronic Crystals, ECRYS99, La Cole-sur-Loup, France*, edited by S. Brazovskii and P. Monceau [J. Phys. IV **9** (1999)].

[3] H. Frölich, Proc. R. Soc. London, Ser. A **223**, 296 (1954); R.E. Peierls, *Quantum Theory of Solids* (Oxford University Press, London, 1955), p. 108; W. Kohn, Phys. Rev. Lett. **2**, 393 (1959).

[4] P. Monceau, in *Electronic Properties of Inorganic Quasi-One-Dimensional Compounds, Part II: Experimental*, edited P. Monceau (Kluwer Academic, Dordrecht, 1985), p. 137 and references therein.

[5] P.M. Williams, G.S. Parry, and C.B. Scruby, Philos. Mag. **29**, 695 (1974); J.A. Wilson, F.J. Di Salvo, and S. Mahajan, Phys. Rev. Lett. **32**, 882 (1974).

[6] H. Fukuyama and H. Takayama, in *Electronic Properties of Inorganic Quasi-One-Dimensional Compounds, Part I: Theoretical*, edited by P. Monceau (Kluwer Academic, Dordrecht, 1985), p. 41, and references therein.

[7] H. Chen and R.M. Fleming, Solid State Commun. **48**, 777 (1983).

[8] R.M. Fleming, R.J. Cava, L.F. Schneemeyer, E.A. Rietman, and R.G. Dunn, Phys. Rev. B **33**, 5450 (1986).

[9] R.J. Cava, R.M. Fleming, P. Littlewood, E.A. Rietman, L.F. Schneemeyer, and R.G. Dunn, Phys. Rev. B **30**, 3228 (1984).

[10] R.J. Cava, R.M. Fleming, R.G. Dunn, and E.A. Rietman, Phys. Rev. B **31**, 8325 (1985).

[11] R.J. Cava, P. Littlewood, R.M. Fleming, R.G. Dunn, and E.A. Rietman, Phys. Rev. B **33**, 2439 (1986).

[12] W.G. Lyons and J.R. Tucker, Phys. Rev. B **40**, 1720 (1989).

[13] L. Sneddon, Phys. Rev. B **29**, 719 (1984).

[14] T. Takoshima, M. Ido, K. Tsutsumi, T. Sambongi, S. Honma, K.

Yamaya, and Y. Abe, Solid State Commun. **35**, 911 (1980).
[15] S.K. Zhilinskii, M.E. Iṭkis, I.Yu. Kal'nova, F.Ya. Nad', and V.B. Preobrazhenskii, Zh. Éksp. Teor. Fiz. **85**, 362 (1983) [Sov. Phys. JETP **58**, 211 (1983)].
[16] F.Ya. Nad' and P. Monceau, Phys. Rev. B **46**, 7413 (1992).
[17] S. Sridhar, D. Reagor, and G. Grüner, Phys. Rev. B **34**, 2223 (1986).
[18] F.Ya. Nad' and P. Monceau, Solid State Commun. **87**, 13 (1993).
[19] F. Nad' and P. Monceau, Phys. Rev. B **51**, 2052 (1995).
[20] W. Higgs and J.C. Gill, Solid State Commun. **47**, 737 (1983).
[21] Z.Z. Wang and N.P. Ong, Phys. Rev. B **34**, 5967 (1986); N.P. Ong and Z.Z. Wang, in *Nonlinearity in Condensed Matter, Proceedings of the Sixth Annual Conference*, edited by A.R. Bishop, D.K. Campbell, P. Kumar, and S.E. Trullinger (Springer-Verlag, Berlin, 1987), p. 350.
[22] V.Y. Pokrovskii, S.V. Zaitsev-Zotov, and F.Ya Nad', J. Phys.: Condens. Matter **5**, 9317 (1993).
[23] V.Y. Pokrovskii and S.V. Zaitsev-Zotov, Phys. Rev. B **61**, 13 261 (2000).
[24] T.A. Davis, W. Schaffer, M.J. Skove, and E.P. Stillwell, Phys. Rev. B **39**, 10 094 (1989).
[25] W. Higgs, in *Charge Density Waves in Solids: Proceedings of the International Conference*, edited by G. Hutiray and J. Solyom (Springer-Verlag, Berlin, 1985), p. 422.
[26] Zhang Dian-lin, Lin Shu-yuan, B.J. Jin, and C.W. Chu, Phys. Rev. B **37**, 4502 (1988).
[27] X. Zhan and J.W. Brill, Synth. Met. **103**, 2671 (1999).
[28] M.E. Itkis, F.Ya. Nad, and P. Monceau, J. Phys.: Condens. Matter **2**, 8327 (1990).
[29] S.V. Zaitsev-Zotov, Phys. Rev. Lett. **71**, 605 (1993).
[30] S.V. Zaitsev-Zotov, G. Remenyi, and P. Monceau, Phys. Rev. B **56**, 6388 (1997).
[31] N.I. Baklanov and S.V. Zaitsev-Zotov, Pis'ma Zh. Éksp. Teor. Fiz. **61**, 656 (1995) [JETP Lett. **61**, 676 (1995)].
[32] N.I. Baklanov, S.V. Zaitsev-Zotov, V.V. Frolov, and P. Monceau, Phys. Lett. A **251**, 340 (1999).
[33] K. Biljaković, J.C. Lasjaunias, P. Monceau, and F. Levy, Europhys. Lett. **8**, 771 (1989).
[34] K. Biljaković, J.C. Lasjaunias, P. Monceau, and F. Levy, Phys. Rev. Lett. **67**, 1902 (1991).
[35] K. Biljaković, in *Phase Transitions and Relaxation in Systems with Competing Energy Scales*, Vol. 415 of *NATO Advanced Study Institute, Series C*, edited by T. Riste and D. Sherrington (Kluwer Academic, Dordrecht, 1993), p. 339.
[36] R.J. Cava, R.M. Fleming, R.G. Dunn, E.A. Rietman, and L.F. Schneemeyer, Phys. Rev. B **30**, 7290 (1984).
[37] J.P. Stokes, M.O. Robbins, and S. Bhattacharya, Phys. Rev. B **32**, 6939 (1985).
[38] K.S. Cole and R.H. Cole, J. Chem. Phys. **9**, 341 (1941); C.J.F. Böttcher and P. Bordewijk, *Theory of Electric Polarisation* (Elsevier, Amsterdam, 1978), Vol. 2.
[39] Wei-yu Wu, A. Janossy, and G. Grüner, Solid State Commun. **49**, 1013 (1984).
[40] A. Kudlik *et al.*, J. Non-Cryst. Solids **235–237**, 406 (1998).
[41] Activated growth $\tau = \tau_0 e^{E_0/T}$, Vogel-Fulcher phenomenological law $\tau = \tau_0 e^{E_0/(T-T_c)}$ (points to the finite freezing temperature).
[42] C.A. Angell, J. Non-Cryst. Solids **131-133**, 13 (1991).
[43] T. Nakayama and N. Sato, J. Phys.: Condens. Matter **10**, L41 (1998) and references therein.
[44] G. Mihaly, T.W. Kim, and G. Grüner, Phys. Rev. B **39**, 13 009 (1989).
[45] A.P. Sokolov, A. Kisliuk, M. Soltwisch, and D. Quitmann, Phys. Rev. Lett. **69**, 1540 (1992).
[46] A. Zettl, G. Grüner, and A.H. Thompson, Phys. Rev. B **26**, 5760 (1982).
[47] S.M. DeLand, G. Mozurkewich, and L.D. Chapman, Phys. Rev. Lett. **66**, 2026 (1991).
[48] B. Hennion, J.P. Pouget, and M. Sato, Phys. Rev. Lett. **68**, 2374 (1992).
[49] K. Jonscher, *Dielectric Relaxation in Solids* (Chelsea Dielectrics, London, 1983).
[50] J. Wiedersich, T. Blochowicz, S. Benkhof, A. Kudlik, N.V. Surovtsev, C. Tschirwitz, V.N. Novikov, and E. Rössler, J. Phys.: Condens. Matter **11**, A147 (1999).
[51] Z.Z. Wang, H. Salva, P. Monceau, M. Renard, C. Rouceau, A. Ayroles, F. Levy, L. Guemas, and A. Meerschaut, J. Phys. (France) **44**, L-311 (1983).
[52] P.B. Littlewood, Phys. Rev. B **36**, 3108 (1987).
[53] S.N. Artemenko and A.F. Volkov, in *Charge Density Waves in Solids*, edited by L. Gor'kov and G. Grüner (North-Holland, New York, 1989), p. 365.
[54] T. Baier and W. Wonneberger, Z. Phys. B **79**, 211 (1990).
[55] W. Aichmann and W. Wonneberger, Z. Phys. B **84**, 375 (1991).
[56] A. Larkin and S. Brazovskii, Solid State Commun. **93**, 275 (1995).
[57] A.F. Volkov, Phys. Lett. A **182**, 433 (1993).
[58] R. Böhmer *et al.*, J. Non-Cryst. Solids **235-237**, 1 (1998).
[59] R.V. Chamberlin, Phys. Rev. Lett. **82**, 2520 (1999).
[60] M.J. Rice, A.R. Bishop, J.A. Krumhansl, and S.E. Trullinger, Phys. Rev. Lett. **36**, 432 (1976).
[61] S.N. Artemenko, F. Gleisberg, and W. Wonneberger. J. Phys. IV **9**, 101 (1999).
[62] S.N. Artemenko and F. Gleisberg, Phys. Rev. Lett. **75**, 497 (1995).
[63] R.H. McKenzie and J.W. Wilkins, Phys. Rev. Lett. **69**, 1085 (1992).
[64] T. Nattermann, Phys. Rev. Lett. **64**, 2454 (1990).
[65] S.K. Zhilinskii, M.E. Itkis, and F. Ya. Nad, Phys. Status Solidi A **81**, 367 (1984).
[66] K.L. Ngai, R.W. Rendell, and H. Jain, Phys. Rev. B **30**, 2133 (1984).
[67] R. Richert and R. Böhmer, Phys. Rev. Lett. **83**, 4337 (1999).
[68] Yu.N. Ovchinnikov, K. Biljakovic, J.C. Lasjaunias, and P. Monceau, Europhys. Lett. **34**, 645 (1996).
[69] A. Larkin, Zh. Éksp. Teor. Fiz. **105**, 1793 (1994) [JETP **78**, 971 (1994)].
[70] S. Brazovskii, in *Les Houches 95*, edited by C. Schlenker J. Dumas, M. Greenblatt, and S. van Smaalen (Plenum Press, New York, 1996), p. 465.
[71] S. Brazovskii, A. Larkin, J. Phys. IV **9**, Pr10-77 (1999).
[72] K. Hosseini, W. Brütting, M. Schwörer, D. Starešinić, K. Biljaković, E. Riedel, S. van Smaalen, and T. Sambongi (unpublished).